

PERFECT DISCRETIZATIONS OF DIFFERENTIAL OPERATORS

SIMON HAUSWIRTH

*Institute for Theoretical Physics, University of Bern,
Sidlerstrasse 5, 3012 Bern, Switzerland
E-mail: simon.hauswirth@itp.unibe.ch*

In this paper we investigate an approach for the numerical solution of differential equations which is based on the perfect discretization of actions. Such perfect discretizations show up at the fixed points of renormalization group transformations. This technique of integrating out the high momentum degrees of freedom with a path integral has been mainly used in lattice field theory, therefore our study of its application to PDE's explores new possibilities. We calculate the perfect discretized Laplace operator for several non-trivial boundary conditions analytically and numerically. Then we construct a parametrization of the perfect Laplace operator and we show that with this parametrization discretization errors – or computation time – can be reduced dramatically compared to the standard discretization.

Keywords: Partial Differential Equations, Boundary Value Problems, Renormalization Group Methods

1. Introduction

It is a standard procedure to introduce a discretized space-time in the numerical study of physical problems. This is the case in quantum field theories where the numerical simulations are performed on a space-time lattice, or in classical field theories (hydrodynamics, electrodynamics etc.), where the corresponding partial differential equations can be discretized. The underlying mesh has a finite lattice spacing a introducing a discretization error whose size depends on a/ξ , where ξ is a typical length scale of the problem. This systematical error is influenced by the discretized form of the differential operators. For example, the standard nearest-neighbor discretization of the Laplace operator has an $\mathcal{O}(a^2)$ error. By adding additional couplings this error can be reduced to $\mathcal{O}(a^4)$, which makes it easier to perform the continuum limit $a \rightarrow 0$. In principle, the discretization error can be eliminated order by order this way, but the resulting Laplace operator would not have much practical value in general: it would become a broad, non-local operator.

The notion of locality will play an important role in the following. We shall call a discretized differential operator local if the size of the region R where the couplings are significantly different from zero goes to zero relative to the typical length scale ξ of the problem in the continuum limit: $R/\xi \rightarrow 0$ ($a \rightarrow 0$). The standard nearest-neighbor discretization of the Laplace operator is obviously local. Similarly, a lattice difference operator whose couplings decay exponentially $\propto e^{-\gamma r}$ with the distance r between the connected points, where $\gamma a = \mathcal{O}(1)$, is local also. In this case $R/\xi \propto 1/(\gamma\xi) \propto a/\xi \rightarrow 0$ in the continuum limit.

Is it possible to construct “perfect” discretized differential operators, i.e. operators which are local and lead to differential equations on the lattice whose solution is free of discretization errors even if a/ξ is not small and thus the resolution is bad? The answer is yes. The problem is related to the existence of perfect lattice actions of classical field theories¹. The Euler-Lagrange equations corresponding to such actions are perfect difference equations in the sense discussed above. Their existence and the technical way of constructing them follows directly from Wilson’s renormalization group (RG) theory². Perfect classical actions were constructed and tested not only for free field theories like the scalar field³, but also for such non-trivial cases like the non-linear σ -model^{4,5}, Yang-Mills gauge theory^{6,7} or the Schwinger model^{8,9,10}. These results might open new paths in the numerical study of partial differential equations. The first attempt in this direction has been made by Katz and Wiese for fluid dynamics¹¹. Although the latter problem seems to be simpler than those treated before, there are new difficulties here — among them the influence of non-trivial boundary conditions. Consider the following simple example: the potential energy of a massive membrane fixed to a frame at its boundary. This is a good problem for testing, as it can be solved analytically for a square frame of size $L \times L$ and therefore the exact solution is known. The standard procedure to solve this problem numerically is to define a lattice and calculate the amplitude of the membrane at the lattice points using the standard discretization of the Laplace operator. However, if a/L is not very small, the results will be far from the exact value due to the large discretization error. To get acceptable results, one needs to go to very fine lattices, that is to very high resolution. On the other hand, as we mentioned, the perfect lattice Laplace operator gives the exact value for the quantity we are looking for at any lattice size, at any resolution, even when the lattice consists of only one point. For the boundary conditions mentioned above, the perfect Laplace operator can even be found analytically.

So far, this is theoretical. For practical calculations, one should use a truncated operator which is easy to handle. For example, one might consider only nearest-neighbor and next-to-nearest-neighbor couplings between lattice points. A boundary will then influence these couplings. Such a truncation only works when the neglected couplings are small, that is when the operator is local. If the influence of the boundary is also local, a parametrization could be constructed which can be used for arbitrary boundary shapes. In this paper, we construct and test such a

parametrization. Let us summarize the problems addressed:

- How do non-trivial boundary conditions affect the perfect Laplace operator?
- Can we truncate and parametrize a perfect difference operator in a way that it is useful for practical purposes?
- Is the improvement we achieve for specific results when using a parametrized perfect operator worth the effort?

As this is a field practically untouched, we turn to the basic problems first. We will see that there the concept of perfect actions leads to excellent results.

2. Renormalization Group Transformations and Perfect Actions

Let us first give a brief review of the construction of perfect actions. Consider a theory described by an action $\mathcal{A}(\phi_n)$, where ϕ_n is the d -dimensional field variable at the lattice point $n = (n_1, \dots, n_d)$. On this lattice, form blocks of 2^d points each. For every block, define a blocked field variable

$$\chi_{n_B} = b \frac{1}{2^d} \sum_{n \in n_B} \phi_n. \quad (2.1)$$

If the original lattice spacing has been a , the blocked field χ_{n_B} lives on a lattice with spacing $2a$. A Renormalization Group transformation (RGT) step leads to a new action $\mathcal{A}'(\chi)$ for the blocked variable by integration over the original field variables ϕ_n :

$$e^{-\mathcal{A}'(\chi)} = \prod_n \int d\phi_n \prod_{n_B} \delta(\chi_{n_B} - b \frac{1}{2^d} \sum_{n \in n_B} \phi_n) e^{-\mathcal{A}(\phi)}. \quad (2.2)$$

It remains to rescale the unit of length in order to keep physical length scales unchanged. After such an RGT step, our theory still describes the same long-distance behaviour, i.e. the same physics. But we have reduced the number of degrees of freedom, that is the number of space-time variables, by a factor of 2^d . On the other hand, the form of the action has changed. Iterating this transformation, one gets coarser and coarser lattices without adding new discretization errors.

An interesting property of RG transformations is the occurrence of fixed points. Most generally, the action of a theory consists of all kinds of interactions and can be written as a sum of interaction terms $\theta_i(\phi)$, $i = 1, 2, \dots$

$$\mathcal{A}(\phi) = \sum_i K_i \theta_i(\phi), \quad (2.3)$$

where K_i are the respective coupling constants. As we said, a RG transformation changes the form of the action, so repeated transformations generate a flow in coupling constant space

$$\{K_i^{(1)}\} \rightarrow \{K_i^{(2)}\} \rightarrow \{K_i^{(3)}\} \rightarrow \dots \quad (2.4)$$

A fixed point occurs if the set of coupling constants remains unchanged under a RG transformation $\{K_i^{(n)}\} = \{K_i^{(n+1)}\} \doteq \{K_i^*\}$. The fixed point action, which we designate by an asterisk, is then defined as

$$\mathcal{A}^*(\phi) = \sum_i K_i^* \theta_i(\phi), \quad (2.5)$$

and depends on the explicit form of the RG transformation. The fixed point action has the beautiful property of being classically perfect: It reproduces all the important classical properties of the continuum action¹.

Now let us consider an example: The perfect Laplace operator Δ^* on a d -dimensional space-time without boundaries can be calculated from the fixed point action of a free real scalar field with the continuum action

$$\mathcal{A}(\phi) = \frac{1}{2} \int d^d x \partial_\mu \phi(x) \partial_\mu \phi(x). \quad (2.6)$$

The equation of motion for this action is the Laplace equation. A general discretization of the action (2.6) contains terms which couple the field at one lattice site to the field at another one:

$$\mathcal{A}(\phi) = \frac{1}{2} \sum_{n,r} \phi_n \rho(r) \phi_{n+r}, \quad (2.7)$$

with the coupling constants $\rho(r)$, $r = (r_1, \dots, r_d)$. For the standard Laplacian in two dimensions, $\rho(0) = 4$ and $\rho(r) = -1$ ($\forall |r| = 1$). We generalize the block transformation in (2.2) and write

$$c \cdot e^{-\mathcal{A}'(\chi)} = \prod_n \int d\phi_n e^{-\mathcal{A}(\phi) - \mathcal{T}(\chi, \phi)}. \quad (2.8)$$

where c is a normalization constant and $\mathcal{T}(\chi, \phi)$ is the blocking kernel

$$\mathcal{T}(\chi, \phi) = 2\kappa \sum_{n_B} (\chi_{n_B} - b \cdot \frac{1}{2^d} \sum_{n \in n_B} \phi_n)^2. \quad (2.9)$$

The parameter κ gives us the possibility to optimize the fixed point action for locality. For $\kappa \rightarrow \infty$, this RG transformation goes over to the one in Eq. (2.2). The fixed point of Eq. (2.8) can be calculated analytically^{12,13}. In momentum space, the inverse of $\rho^*(q)$ is

$$\frac{1}{\tilde{\rho}^*(q)} = \sum_{l \in \mathbb{Z}^d} \frac{1}{(q + 2\pi l)^2} \prod_\mu \frac{\sin^2(\frac{q_\mu}{2} + \pi l_\mu)}{(\frac{q_\mu}{2} + \pi l_\mu)^2} + \frac{1}{3\kappa}. \quad (2.10)$$

The fixed point Laplacian $(\Delta^* \phi)_n = -\sum_r \rho^*(r) \phi_{n+r}$ is then calculated numerically by Fourier transforming $\tilde{\rho}^*(q)$. A thorough examination of different blocking kernels¹⁴ has shown that the kernel (2.9) with $\kappa = 2$ gives very good results in terms

of locality: The couplings $\rho(r)$ decay exponentially $\propto e^{-\gamma r}$ with a large decay coefficient $\gamma \approx 3.5$. For $d = 2$, we get the translationally invariant perfect Laplacian on a plane, which we will use in the next section.

3. Perfect Laplacian for a Square Boundary

The perfect Laplace operator calculated above only holds in the absence of boundaries. So let us now introduce non-trivial boundary conditions: Restrict the field ϕ to a square area in two dimensions with $\phi = 0$ on the boundaries. In the presence of boundaries, the perfect Laplacian $\rho^*(n, n')$ will no longer be translation invariant. In this section we present two ways of calculating the perfect Laplacian for these boundary conditions. First we explicitly perform the RG transformation, leading to an analytical expression for the perfect Laplacian, and second we show how to find $\rho^*(n, n')$ as a function of the translationally invariant perfect Laplacian $\rho^*(r)$, which is already known from (2.10). The latter procedure will lead to an elegant way of avoiding possible normalization problems when truncating the couplings.

3.1. Explicit RG Transformation

Consider a square box with side length L in $d = 2$. In the continuum, the action of a free scalar field is

$$\mathcal{A}(\phi) = \frac{1}{2} \int_0^L d^2x \partial_\mu \phi(x) \partial_\mu \phi(x). \quad (2.11)$$

For the calculation of the fixed point action, we will work in Fourier space. Our ansatz is to use a Fourier transformation

$$\phi(x) = \frac{1}{L^2} \sum_q \Psi_q(x) \tilde{\phi}(q), \quad (2.12)$$

with orthonormal basis functions $\Psi_q(x) = 2 \sin(q_1 x_1) \sin(q_2 x_2)$ which ensure that the field ϕ fulfills the boundary conditions. The momentum variable $q = (q_1, q_2)$ takes the discrete set of values $q_i = k_i \pi / L$ with $k_i = 1, 2, \dots, \infty$ ($i = 1, 2$). In momentum space, the action (2.11) reads

$$\mathcal{A}(\tilde{\phi}) = \frac{1}{2L^2} \sum_q q^2 \tilde{\phi}(q) \tilde{\phi}(q). \quad (2.13)$$

As shown in Fig. 1, we define the lattice points n_i at half-integer values of the continuum space variable $x_i = (n_i + 1/2)a$ with $0 \leq x_i < L = Na$. Performing the RG transformation (2.8), (2.9) on this lattice, we arrive at a coarser lattice with lattice unit $2a$, defined in the middle of the dashed blocks in Fig. 1. Consider the correlation function

$$\langle \phi_{n'} \phi_{n''} \rangle = \frac{1}{Z} \prod_n \int d\phi_n e^{-\mathcal{A}(\phi)} \phi_{n'} \phi_{n''}, \quad (2.14)$$

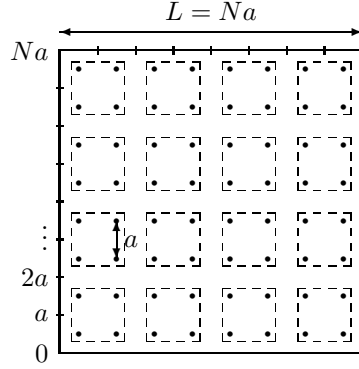


Figure 1: The $N \times N$ -lattice in an area with square boundaries. The blocking kernel (2.9) connects the four fine lattice points inside a dashed box to one coarse lattice point in the center of the box.

where Z is the partition function and assume $\mathcal{A} = \mathcal{A}^*$. From Eq. (2.8) follows that the correlation functions on the coarse and fine lattices are related by

$$\langle \chi_{n_B} \chi_{n'_B} \rangle = \left(\frac{1}{4}\right)^2 \sum_{n \in n_B} \sum_{n' \in n'_B} \langle \phi_n \phi_{n'} \rangle + \frac{1}{4\kappa} \delta_{n_B n'_B}. \quad (2.15)$$

Iterating this transformation an infinite number of times leads to a relation between the correlation functions on the original lattice with lattice unit a and the one in the continuum. (As we need no longer two lattice field variables, we replace the coarse lattice variable χ_{n_B} by our standard lattice notation ϕ_n again.)

$$\langle \phi_n \phi_{n'} \rangle = \int_0^1 d^2x \int_0^1 d^2x' \langle \phi((n+x)a) \phi((n'+x')a) \rangle + \frac{1}{3\kappa} \delta_{nn'}. \quad (2.16)$$

On the right hand side, we insert the continuum free field propagator

$$\langle \phi(x) \phi(y) \rangle = \frac{1}{L^2} \sum_q \Psi_q(x) \Psi_q(y) \frac{1}{q^2}, \quad (2.17)$$

which follows from (2.13), with $x_i, y_i \in (0, L)$. Setting the lattice unit $a = 1$ and performing the definite integration over x and x' gives

$$\langle \phi_n \phi_{n'} \rangle = \frac{4}{N^2} \sum_q \prod_{i=1}^2 \sin(q_i(n_i + \frac{1}{2})) \sin(q_i(n'_i + \frac{1}{2})) \prod_{i=1}^2 \frac{(\sin \frac{q_i}{2})^2}{(\frac{q_i}{2})^2} \frac{1}{q^2} + \frac{1}{3\kappa} \delta_{nn'}. \quad (2.18)$$

After a few algebraic steps, we can bring this into the following form:

$$\langle \phi_n \phi_{n'} \rangle = \frac{1}{N^2} \sum_Q \Psi_Q(n) \Psi_Q(n') \cdot \sum_{l=-\infty}^{\infty} \frac{1}{(Q + 2\pi l)^2} \prod_{i=1}^2 \frac{\sin^2 \frac{Q_i}{2}}{(\frac{Q_i}{2} + \pi l_i)^2} + \frac{1}{3\kappa} \delta_{nn'}, \quad (2.19)$$

with $\Psi_Q(n) = \xi_{Q_1}(n_1) \cdot \xi_{Q_2}(n_2)$, and

$$\xi_{Q_i}(n_i) = \begin{cases} \sqrt{2} \sin(Q_i(n_i + \frac{1}{2})) & , Q_i \neq \pi, \\ \sin(Q_i(n_i + \frac{1}{2})) & , Q_i = \pi. \end{cases} \quad (2.20)$$

The new momentum variable Q is restricted to the Brillouin zone and takes the values $Q_i = k_i \pi / N$, $k_i = 1, \dots, N$. The result (2.19) provides us the fixed point propagator in momentum space

$$\frac{1}{\rho^*(Q)} = \sum_{l=-\infty}^{\infty} \frac{1}{(Q + 2\pi l)^2} \prod_{i=1}^2 \frac{\sin^2 \frac{Q_i}{2}}{(\frac{Q_i}{2} + \pi l_i)^2} + \frac{1}{3\kappa}. \quad (2.21)$$

Perform the Fourier transformation

$$\rho^*(n, n') = \frac{1}{N^2} \sum_Q \Psi_Q(n) \Psi_Q(n') \cdot \rho^*(Q), \quad (2.22)$$

to get the couplings of the fixed point action $\mathcal{A}^*(\phi) = 1/2 \sum_{n, n'} \rho^*(n, n') \phi_n \phi_{n'}$ in configuration space ($n_i = 0, 1, \dots, N - 1$). In contrast to the situation on an unbounded lattice, $\rho^*(n, n')$ is no longer translationally invariant; it does not depend only on the distance $r = n' - n$ as the couplings in Eq. (2.7). Consequently, we have a different $\rho^*(n, r)$ for every lattice point n . On the other hand we expect — and it is really the case, as we will show — that away from the boundaries the difference between $\rho^*(n, r)$ and the perfect Laplacian of the translationally invariant case $\rho^*(r)$ goes to zero exponentially with the distance from the boundary, which will be a crucial property to construct a parametrization.

3.2. Construction from Symmetry Properties

There is another, more elegant way to find the perfect Laplacian for a square region with zero boundary conditions in $d = 2$. The translationally invariant perfect Laplacian $\rho^*(r)$ (2.10) is already known, and we show that this knowledge can be used to solve the problem with these non-trivial boundary conditions. As a boundary, consider a single wall at $x_1 = 0$ first where the field ϕ has to vanish. We extend the field beyond the boundary and introduce the condition

$$\phi(-x_1, x_2) = -\phi(x_1, x_2), \quad (2.23)$$

which implies $\phi = 0$ on the boundary. For the lattice field, we have $\phi_{-n_1-1, n_2} = -\phi_{n_1, n_2}$, as the lattice points n are at half-integer values of $x = n + 1/2$. Using this symmetry relation and the symmetry property $\rho^*(-r_1, r_2) = \rho^*(r_1, r_2)$, we rewrite the perfect Laplace equation on the unbounded lattice into an equation on the right halfplane:

$$\begin{aligned} \sum_r \rho^*(r) \phi_{n+r} &= \sum_{r_2} \left[\sum_{r_1 \geq 0} \rho^*(r-n) \phi_r + \sum_{r_1 < 0} \rho^*(r-n) \phi_r \right] \\ &= \sum_{r_2} \sum_{r_1 \geq 0} [\rho^*(r-n) - \rho^*(r_1 + n_1 + 1, r_2 - n_2)] \phi_r. \end{aligned} \quad (2.24)$$

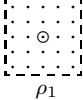
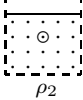
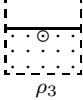
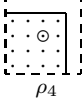
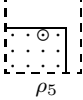
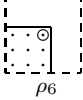
 ρ_1	$\rho_1(r_1, r_2)$	$r_1 = -2$	$r_1 = -1$	$r_1 = 0$	$r_1 = 1$	$r_1 = 2$
	$r_2 = 2$	0.00162	-0.00068	-0.00200	-0.00068	0.00162
	$r_2 = 1$	-0.00068	-0.19024	-0.61773	-0.19024	-0.00068
	$r_2 = 0$	-0.00200	-0.61773	3.23881	-0.61773	-0.00200
	$r_2 = -1$	-0.00068	-0.19024	-0.61773	-0.19024	-0.00068
	$r_2 = -2$	0.00162	-0.00068	-0.00200	-0.00068	0.00162
 ρ_2	$\rho_2(r_1, r_2)$	$r_1 = -2$	$r_1 = -1$	$r_1 = 0$	$r_1 = 1$	$r_1 = 2$
	$r_2 = 2$	0.00000	0.00000	0.00000	0.00000	0.00000
	$r_2 = 1$	-0.00230	-0.18956	-0.61573	-0.18956	-0.00230
	$r_2 = 0$	-0.00200	-0.61773	3.23881	-0.61773	-0.00200
	$r_2 = -1$	-0.00068	-0.19024	-0.61773	-0.19024	-0.00068
	$r_2 = -2$	0.00162	-0.00068	-0.00200	-0.00068	0.00162
 ρ_3	$\rho_3(r_1, r_2)$	$r_1 = -2$	$r_1 = -1$	$r_1 = 0$	$r_1 = 1$	$r_1 = 2$
	$r_2 = 2$	0.00000	0.00000	0.00000	0.00000	0.00000
	$r_2 = 1$	0.00000	0.00000	0.00000	0.00000	0.00000
	$r_2 = 0$	-0.00132	-0.42749	3.85654	-0.42749	-0.00132
	$r_2 = -1$	-0.00230	-0.18956	-0.61573	-0.18956	-0.00230
	$r_2 = -2$	0.00162	-0.00068	-0.00200	-0.00068	0.00162
 ρ_4	$\rho_4(r_1, r_2)$	$r_1 = -2$	$r_1 = -1$	$r_1 = 0$	$r_1 = 1$	$r_1 = 2$
	$r_2 = 2$	0.00000	0.00000	0.00000	0.00000	0.00000
	$r_2 = 1$	-0.00230	-0.18956	-0.61573	-0.18726	0.00000
	$r_2 = 0$	-0.00200	-0.61773	3.23881	-0.61573	0.00000
	$r_2 = -1$	-0.00068	-0.19024	-0.61773	-0.18956	0.00000
	$r_2 = -2$	0.00162	-0.00068	-0.00200	-0.00230	0.00000
 ρ_5	$\rho_5(r_1, r_2)$	$r_1 = -2$	$r_1 = -1$	$r_1 = 0$	$r_1 = 1$	$r_1 = 2$
	$r_2 = 2$	0.00000	0.00000	0.00000	0.00000	0.00000
	$r_2 = 1$	0.00000	0.00000	0.00000	0.00000	0.00000
	$r_2 = 0$	-0.00132	-0.42749	3.85654	-0.42617	0.00000
	$r_2 = -1$	-0.00230	-0.18956	-0.61573	-0.18726	0.00000
	$r_2 = -2$	0.00162	-0.00068	-0.00200	-0.00230	0.00000
 ρ_6	$\rho_6(r_1, r_2)$	$r_1 = -2$	$r_1 = -1$	$r_1 = 0$	$r_1 = 1$	$r_1 = 2$
	$r_2 = 2$	0.00000	0.00000	0.00000	0.00000	0.00000
	$r_2 = 1$	0.00000	0.00000	0.00000	0.00000	0.00000
	$r_2 = 0$	-0.00132	-0.42617	4.28403	0.00000	0.00000
	$r_2 = -1$	-0.00230	-0.18726	-0.42617	0.00000	0.00000
	$r_2 = -2$	0.00162	-0.00230	-0.00132	0.00000	0.00000

Table 1: The normalized, truncated couplings of the perfect Laplacian for points far from boundaries (ρ_1), for points near a wall (ρ_2, ρ_3) and near a convex corner (ρ_4, ρ_5, ρ_6). In the small image on the left, the lattice point n is denoted by a circle, and all the sites in the 2-hypercube around n which lie inside the boundary are shown as small dots. The table on the right shows the values of the (r_1, r_2) -coupling for the lattice point n . The couplings for ρ_2 - ρ_6 are made up from ρ_1 with the construction explained in the text.

This defines a perfect Laplace operator with $\phi = 0$ on the second axis, that is the perfect Laplacian near a wall

$$\rho^*(n, r) = \rho^*(r) - \rho^*(r_1 + 2n_1 + 1, r_2), \quad (2.25)$$

where n_1 is the distance from the wall. The variables n and $n' = n + r$ are here restricted to the area inside the boundary which is the positive halfplane in the first coordinate.

Now consider a boundary of two walls at $x_1 = 0$ and $x_2 = 0$ forming a corner. In the Laplace equation, the sum over the lattice points can be split into sums over the four quadrants of the plane. Proceeding as in the above case for a wall, we get the perfect Laplacian

$$\begin{aligned} \rho^*(n, r) = \rho^*(r) - \rho^*(r_1 + 2n_1 + 1, r_2) - \rho^*(r_1, r_2 + 2n_2 + 1) \\ + \rho^*(r_1 + 2n_1 + 1, r_2 + 2n_2 + 1), \end{aligned} \quad (2.26)$$

with both n and $n + r$ lying in the first quadrant.

Finally, we may form a square boundary out of four walls at $x_1 = 0$, $x_1 = N$, $x_2 = 0$ and $x_2 = N$. The field outside the boundary is formally defined by periodically mirroring it at the boundary with alternating sign

$$\phi(x_1, x_2) = (-1)^{k_1+k_2} \phi((-1)^{k_1} x_1 + 2l_1 N, (-1)^{k_2} x_2 + 2l_2 N), \quad (2.27)$$

for any $k_i = 0, 1$ and $l_i \in \mathbf{Z}$, ($i = 1, 2$). The sum over the whole plane then splits up into sums over N -squares

$$\sum_r \rho^*(r) \phi_{n+r} = \sum_{i=1}^2 \sum_{l_i \in \mathbf{Z}} \sum_{k_i=0}^1 \sum_{s_i=0}^{N-1} \rho(r-n) \phi_r, \quad (2.28)$$

where the variable r running over the lattice points is given by $r_i = (-1)^{k_i} s_i - k_i + 2l_i N$ for $i = 1, 2$. The perfect Laplacian consists of the infinite sum of couplings

$$\rho^*(n, r) = \sum_{i=1}^2 \sum_{l_i \in \mathbf{Z}} \sum_{k_i=0}^1 (-1)^{k_1+k_2} \rho^*(r_1 + 2k_1 n_1 + k_1 + 2l_1 N, r_2 + 2k_2 n_2 + k_2 + 2l_2 N), \quad (2.29)$$

with both n and $n + r$ lying inside the boundary. A check for a lattice with $N = 1$ shows that the relation (2.29) with the translationally invariant couplings (2.10) gives the same result $\rho^*(0, 0) = 4.95513$ as the explicit RG transformation (2.21), (2.22).

4. Perfect Laplacian near a Concave Corner

For boundary shapes where the fixed point action is hard or impossible to find analytically, RG transformations may be performed numerically. We performed such a numerical RGT in order to find the couplings of the fixed point Laplacian

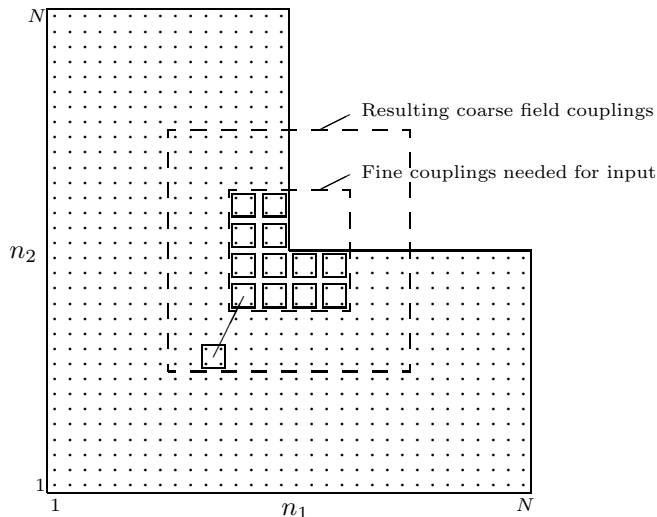


Figure 2: The $N = 32$ - lattice used to calculate the couplings near a concave corner. The couplings between the fine lattice points (shown as dots) have to be fixed. The RG transformation then gives the couplings between the coarse lattice points (denoted by squares) inside the large dashed box, which are used as an input for the fine field couplings inside the small dashed box in the next iteration.

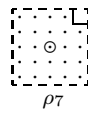
near the concave corner of an L-shaped boundary, that is a square with a smaller square cut out, in $d = 2$ (see Fig. 2). For quadratic actions and blocking kernels, the RG transformation Eq. (2.8) can be written as a minimizing condition for the fine field ϕ :

$$\mathcal{A}'(\chi) = \min_{\phi} [\mathcal{A}(\phi) + \mathcal{T}(\chi, \phi)] + \text{const.} \quad (2.30)$$

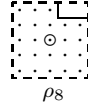
To get close to a fixed point, we have to iterate this RGT step. The results of the previous step — which are the couplings of the resulting coarse action — are then used as an input for the next step, that is as a new starting guess for the fine action $\mathcal{A}(\phi)$. After $\mathcal{O}(20)$ iterations, we find a very close approximation to the couplings of the fixed point action.

We worked on a lattice with $N = 32$, as shown in Fig. 2, and looked for the couplings of the coarse field inside the large dashed box. Outside the small dashed box in Fig. 2, we used in every RGT step the parametrized couplings from Table 1 for the fine action. For the couplings inside the small dashed box, we used the standard Laplacian in the first iteration, and afterwards the result of the previous iteration. For every step, the coarse field couplings can be read out one by one by choosing appropriate coarse field configurations as an input. Our results for the fixed point couplings are listed in Table 2.

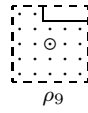
5. Parametrization for Boundaries of Arbitrary Shape



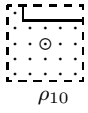
$\rho_7(r_1, r_2)$	$r_1 = -2$	$r_1 = -1$	$r_1 = 0$	$r_1 = 1$	$r_1 = 2$
$r_2 = 2$	0.00160	-0.00072	-0.00192	-0.00206	0.00000
$r_2 = 1$	-0.00071	-0.19033	-0.61787	-0.19145	-0.00206
$r_2 = 0$	-0.00190	-0.61784	3.26307	-0.61787	-0.00192
$r_2 = -1$	-0.00071	-0.19033	-0.61784	-0.19033	-0.00072
$r_2 = -2$	0.00160	-0.00071	-0.00190	-0.00071	0.00160



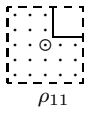
$\rho_8(r_1, r_2)$	$r_1 = -2$	$r_1 = -1$	$r_1 = 0$	$r_1 = 1$	$r_1 = 2$
$r_2 = 2$	0.00160	-0.00071	-0.00043	0.00000	0.00000
$r_2 = 1$	-0.00071	-0.19032	-0.61625	-0.18956	-0.00233
$r_2 = 0$	-0.00190	-0.61787	3.26192	-0.61787	-0.00196
$r_2 = -1$	-0.00071	-0.19033	-0.61784	-0.19033	-0.00072
$r_2 = -2$	0.00160	-0.00071	-0.00190	-0.00071	0.00160



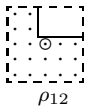
$\rho_9(r_1, r_2)$	$r_1 = -2$	$r_1 = -1$	$r_1 = 0$	$r_1 = 1$	$r_1 = 2$
$r_2 = 2$	0.00160	0.00062	0.00000	0.00000	0.00000
$r_2 = 1$	-0.00071	-0.18948	-0.61637	-0.18963	-0.00233
$r_2 = 0$	-0.00192	-0.61787	3.27774	-0.61788	-0.00196
$r_2 = -1$	-0.00072	-0.19033	-0.61784	-0.19033	-0.00072
$r_2 = -2$	0.00160	-0.00071	-0.00190	-0.00071	0.00160



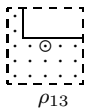
$\rho_{10}(r_1, r_2)$	$r_1 = -2$	$r_1 = -1$	$r_1 = 0$	$r_1 = 1$	$r_1 = 2$
$r_2 = 2$	0.00021	0.00000	0.00000	0.00000	0.00000
$r_2 = 1$	-0.00206	-0.18964	-0.61594	-0.18965	-0.00233
$r_2 = 0$	-0.00196	-0.61788	3.24479	-0.61788	-0.00196
$r_2 = -1$	-0.00072	-0.19033	-0.61784	-0.19033	-0.00072
$r_2 = -2$	0.00160	-0.00071	-0.00190	-0.00071	0.00160



$\rho_{11}(r_1, r_2)$	$r_1 = -2$	$r_1 = -1$	$r_1 = 0$	$r_1 = 1$	$r_1 = 2$
$r_2 = 2$	0.00155	-0.00206	-0.00051	0.00000	0.00000
$r_2 = 1$	-0.00068	-0.18948	-0.46147	0.00000	0.00000
$r_2 = 0$	-0.00186	-0.61625	3.36152	-0.46147	-0.00051
$r_2 = -1$	-0.00076	-0.19145	-0.61625	-0.18948	-0.00206
$r_2 = -2$	0.00161	-0.00076	-0.00186	-0.00068	0.00155



$\rho_{12}(r_1, r_2)$	$r_1 = -2$	$r_1 = -1$	$r_1 = 0$	$r_1 = 1$	$r_1 = 2$
$r_2 = 2$	0.00021	0.00055	0.00000	0.00000	0.00000
$r_2 = 1$	0.00062	-0.02666	0.00000	0.00000	0.00000
$r_2 = 0$	-0.00043	-0.46147	3.88365	-0.42738	-0.00121
$r_2 = -1$	-0.00206	-0.18956	-0.61637	-0.18964	-0.00233
$r_2 = -2$	0.00156	-0.00074	-0.00179	-0.00073	0.00155



$\rho_{13}(r_1, r_2)$	$r_1 = -2$	$r_1 = -1$	$r_1 = 0$	$r_1 = 1$	$r_1 = 2$
$r_2 = 2$	-0.00001	0.00000	0.00000	0.00000	0.00000
$r_2 = 1$	0.00055	0.00000	0.00000	0.00000	0.00000
$r_2 = 0$	-0.00051	-0.42738	3.85640	-0.42757	-0.00121
$r_2 = -1$	-0.00233	-0.18963	-0.61594	-0.18965	-0.00233
$r_2 = -2$	0.00155	-0.00073	-0.00179	-0.00073	0.00155

Table 2: The truncated couplings of the perfect Laplacian near a concave corner. These couplings are the results of the iterative blocking procedure and are therefore not normalized.

The main observation which allows us to construct a reasonable parametrization for the perfect Laplacian that can be used to approximate arbitrarily shaped boundaries is the fact that not only its couplings decay exponentially with the distance, but also the effect of the boundary on the couplings: According to Eq. (2.25), the difference between the perfect Laplacian near a wall and the translationally invariant perfect Laplacian on a plane without boundaries

$$\Delta\rho_n^*(r) \doteq \rho^*(n, r) - \rho^*(r) = -\rho^*(r_1 + 2n_1 + 1, r_2), \quad (2.31)$$

decays with the distance from the wall n_1 at twice the decay rate of the FP Laplacian couplings. The value of the decay constant γ , which is defined by $\Delta\rho_n^*(r) \propto e^{-\gamma \cdot n_1}$, where n_1 denotes the orthogonal distance from the wall — or the diagonal distance from the corner, respectively — is listed for several couplings r near a wall and near a corner in Table 3. This very strong exponential decay means that for points a few

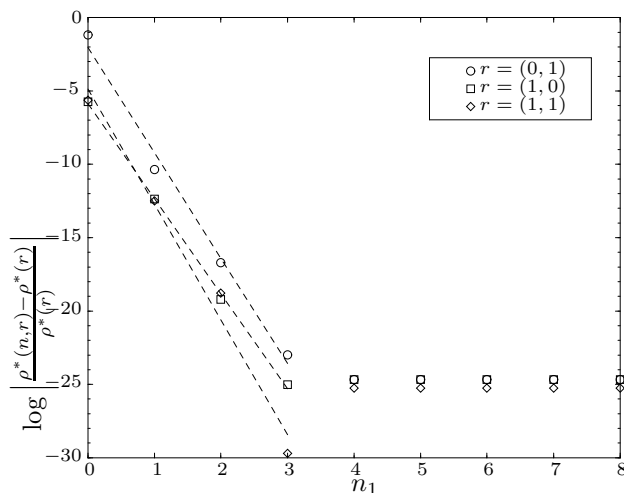


Figure 3: The relative difference $\Delta\rho_n^*(r)/\rho^*(r)$ between three couplings near a wall and the respective couplings of the perfect Laplacian on an infinite lattice. The couplings $\rho^*(n, r)$ are calculated on a lattice with $N = 17$ at the lattice sites $n = (n_1, (N + 1)/2)$. n_1 is therefore the distance from the wall in lattice units. The difference decreases exponentially with the distance from the wall. The slope γ_w is listed in Table 3. For distances larger than 3 lattice units, the difference is already beyond the numerical accuracy.

lattice spacings away from walls, the presence of the boundary influences the fixed point Laplacian at that point only negligibly, and therefore we may parametrize the perfect Laplacian in a way that it can be used for lattices with boundaries of an arbitrary shape.

r	$\gamma^{(wall)}$	$\gamma^{(corner)}$
(0,1)	7.2	7.2
(1,0)	6.5	7.2
(1,1)	7.8	7.0
(0,2)	5.9	6.0

Table 3: The exponential decay rate γ for the effect of the boundary on different couplings. The values are from linear least-squares fits to the first few data points in Figure 3.

In our parametrization, we take together points with very similar $\rho^*(n, r)$ (e.g. all the points with a distance from the boundary of more than one lattice unit) and use the same operator $\rho_m(r)$ for all these points. Thus, we classify the lattice points by their position relative to the boundary (lower left corner, right wall, ...) and define a set of operators $\rho_m(r)$, $m = 1, \dots, 13$, where m is the type of lattice point as shown in Fig. 4. Making this approximation, our set of operators is no longer perfect, and so we have dropped the asterisk in the notation.

	3	5	6
	2	4	
	1		

Figure 4: Point types used for the parametrization. The lattice points are classified by their relative position to the boundary. For every point type m we define a different Laplace operator $\rho_m(r)$ (see Table 1). The definition of ρ_7, \dots, ρ_{13} is shown in Table 2.

5.1. Truncation and Normalization

For practical purposes, the perfect Laplacian must be truncated to a finite number of couplings. The most primitive nearest-neighbor Laplace operator and its simple improved versions have the basic property that they all approach the same exact continuum result as the resolution is increased (universality). We have to ensure that our approximate truncated perfect Laplace operator also has this basic property. This can be achieved when imposing some conditions implied by elementary principles on our parametrized action. Let us consider the case of an unbounded lattice first. Any discretized action should describe the physical properties of the continuum action. For example, the spectrum of the discretized action, which is given by the poles of the propagator, has to go over to the spectrum of the continuum action. In the continuum, the free field propagator is q^{-2} , and the poles are at $q = (p, i|p|)$. The relativistic dispersion relation in two euclidian dimensions is

$E(k) = -iq_2 = |p|$. The propagator $1/\rho(q)$ of a quadratic discretized action should have the same poles, therefore the couplings have to fulfill the sum rule

$$S_0 = \sum_{r_1, r_2} \rho(r_1, r_2) = 0. \quad (2.32)$$

Furthermore, we demand that the lattice action takes the form of the continuum action for small momenta q , that is $\lim_{q \rightarrow 0} \rho(q) = q^2$. This leads to the sum rule

$$S_2 = \sum_{r_1, r_2} (r_1^2 + r_2^2) \cdot \rho(r_1, r_2) = -4. \quad (2.33)$$

When we have boundaries, the above considerations can't be used directly to find sum rules. But with a different approach, we can at least find some conditions for the couplings. Consider a wall at $x_1 = 0$. The field $\phi(x) = x_1$ is a solution to the continuum Laplace equation and is zero at the boundary. Therefore the lattice field $\Phi_n = n_1 + 1/2$ is a solution to the lattice Laplace equation, and when inserting this solution we find a condition for the couplings $\rho_n(r)$:

$$S_1^{(w)} = \sum_{r_1, r_2} \rho_n(r_1, r_2) (r_1 + \frac{1}{2}) = 0. \quad (2.34)$$

For a corner, $\phi(x) = x_1 x_2$ is a solution in the continuum. Hence, the lattice field $\Phi_n = (n_1 + 1/2)(n_2 + 1/2)$ solves the lattice Laplace equation, and the sum rule is

$$S_1^{(c)} = \sum_{r_1, r_2} \rho_n(r_1, r_2) (r_1 + \frac{1}{2})(r_2 + \frac{1}{2}) = 0. \quad (2.35)$$

While (2.34) and (2.35) are trivially fulfilled on an unbounded lattice, they make sense as a normalizing condition for the couplings in the presence of a boundary. We remark that Eq. (2.35) holds for both convex and concave corners.

We construct our parametrization in the following manner: First we normalize the truncated Laplacian for inner points ρ_1 — which we take from Eq. (2.10) — by setting the $(0, 0)$ -coupling properly to get $S_0 = 0$ and by rescaling all couplings to ensure $S_2 = -4$. Then we build the Laplace operators ρ_2, \dots, ρ_6 out of the already corrected couplings of ρ_1 with the help of the relations (2.25) and (2.26). The resulting couplings are listed in Table 1. Together with the couplings near a concave corner ρ_7, \dots, ρ_{13} , we have a parametrization that can be used to approximate any two-dimensional shape.

6. Testing the Parametrization

Let us first check the statement that the fixed point action is classically perfect on an exactly solvable problem. Consider the free scalar field with a constant source f :

$$\mathcal{A}(\phi) = \frac{1}{2} \int_0^L d^2x \partial_\mu \phi(x) \partial_\mu \phi(x) + f \int_0^L d^2x \phi(x). \quad (2.36)$$

We may interpret this as the action of a membrane which is fixed to $\phi = 0$ at the boundaries and has mass density f . The total mass is then $F = fL^2$. The equation of motion to the action (2.36) is the Poisson equation $\Delta\phi(x) = f$. The Green's function to the Laplace operator which fulfills the given boundary conditions is

$$G(x, y) = -\frac{1}{L^2} \sum_q \frac{\Psi_q(x)\Psi_q(y)}{q^2}, \quad (2.37)$$

with $\Psi_q(x) = 2 \sin(q_1 x_1) \sin(q_2 x_2)$ and $q_i = k_i \pi / L$, ($k_i \in \mathbf{N}$). Plugging (2.37) back into (2.36), we can calculate the value of the action and the potential energy $E^{(cont)} = 2\mathcal{A} \simeq -0.035144 \cdot F^2$. For $\kappa \rightarrow \infty$, it is easy to check that the perfect action (2.22) reproduces this continuum result exactly even for $N = 1$, i.e. when the lattice consists of only one single point!

To compare classical quantities like the value of the action on the lattice and in the continuum, we have to take into account the constant c which appears in the RG transformation (2.8). For the fine lattice action

$$\mathcal{A}(\phi) = \frac{1}{2} \sum_{n,r} \rho^*(r) \phi_n \phi_{n+r} + f_\phi \sum_n \phi_n, \quad (2.38)$$

with the perfect Laplace operator $\rho^*(r)$ and constant mass density f_ϕ , we get after one RGT step the coarse lattice action

$$\mathcal{A}(\chi) = \frac{1}{2} \sum_{n_B, r_B} \rho^*(r_B) \chi_{n_B} \chi_{n_B+r_B} + f_\chi \sum_{n_B} \chi_{n_B} - \sum_{n_B} \frac{f_\chi^2}{8\kappa}, \quad (2.39)$$

with $f_\chi = 4f_\phi$. Hence, after iterating to the continuum, the potential energy is calculated from the lattice field configuration $\bar{\phi}$ which solves the perfect Poisson equation by

$$E = f_\phi \sum_n \bar{\phi}_n + \frac{F^2}{3V\kappa}, \quad (2.40)$$

where V denotes the lattice volume.

As a check of the quality of our parametrization of the perfect Laplace operator, we numerically solved the lattice Poisson equation $A\phi = f$ for square boundaries with the standard $(4, -1, -1, -1)$ -Laplacian and with our parametrized Laplace operator made up from ρ_1, \dots, ρ_6 . For the resulting field configuration, we determined the potential energy $E = f \sum_n \bar{\phi}_n^{(std)}$ for the field configuration $\bar{\phi}^{(std)}$ computed with the standard Laplacian and (2.40) for the configuration $\bar{\phi}^{(pp)}$ computed with the parametrized perfect Laplacian. Fig. 5 shows a plot of the relative error $(E - E^{(cont)})/E^{(cont)}$ as a function of the inverse lattice volume $1/N^2$. The error for our parametrization is proportional to $1/N^2$ and is for any lattice size smaller by a factor of about 180 than the error of the standard Laplacian. This factor can probably still be increased by tuning the normalization procedure of the truncated couplings. Fig. 6 shows what happens when the couplings are not normalized and therefore do not fulfill the sum rules S_0 and S_2 . We see that the error

is then no longer proportional to the inverse lattice size. While for coarse lattices — that is small N — the error is small, the results get worse for finer lattices, and somewhere a point is reached where the standard Laplacian gets better than the parametrization. If this should be avoided, one has to correct the truncation error.

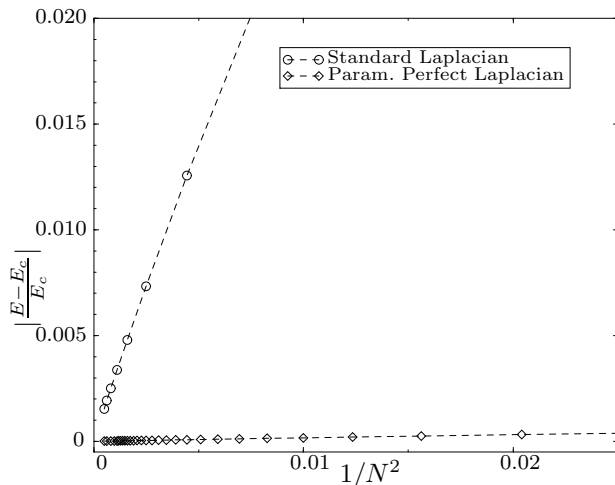


Figure 5: Relative error for the numerical solution of our test problem. The error for the parametrized perfect Laplacian is for any resolution about 180 times smaller than for the standard Laplacian and gives a 0.06% error at $N = 5$. In other words, our parametrization gives better results on a 5^2 lattice than the standard Laplacian on a 74^2 lattice.

Finally, we make the same comparison for L-shaped boundaries as shown in Fig. 2. As above, we solve the lattice Poisson equation with the standard Laplacian and the parametrized perfect Laplacian, for which we take the couplings ρ_1, \dots, ρ_{13} listed in Tables 1 and 2. The lattice volume V for this shape is $V = 3/4N^2$. We compare lattice sizes N between 8 and 72. As we see in Fig. 7, the parametrized perfect Laplacian gives excellent results for any lattice size, while for the standard Laplacian we have to use very fine lattices to get acceptable results. For example, take a lattice with $N = 10$. The standard Laplacian then has an $\mathcal{O}(25\%)$ error, while the error for the parametrized perfect Laplacian is $\mathcal{O}(0.1\%)$.

7. Generalizations

The parametrization presented in the previous sections has some limitations: The boundaries have fixed orientation and are always half a lattice spacing away from the lattice points, and we only used a constant source in the action. In this section we show how to overcome these limitations.

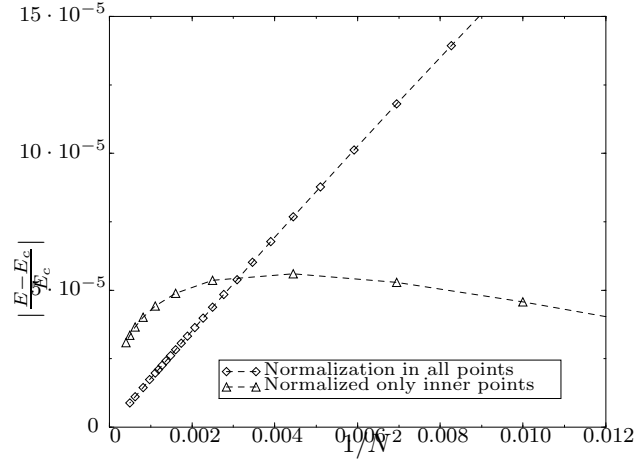


Figure 6: Relative errors for the correctly normalized parametrized perfect Laplacian and for an incompletely normalized parametrization. Although the correct normalization gives somewhat larger errors for small lattices (large lattice unit a), it makes sure that for any lattice size, the results are better than for the standard Laplacian. The error of the standard Laplacian is far beyond the scale of this plot (compare Figure 5).

Consider a RG transformation of the action with a general source term $J(x)$:

$$S_J[\phi] = \frac{1}{2} \int d^d x [\partial_\mu \phi(x) \partial_\mu \phi(x) + J(x) \phi(x)]. \quad (2.41)$$

Blocking out of continuum ^{15,7,8} with the kernel

$$T_\kappa[\Phi, \phi] = \kappa \sum_n \left(\Phi_n - \int d^d x \omega(x-n) \phi(x) \right)^2, \quad (2.42)$$

where $\omega(x)$ is an arbitrary blocking function gives the the result in Fourier space

$$\mathcal{A}[\Phi] = \frac{1}{2} \int_{-\pi}^{\pi} \frac{d^d k}{(2\pi)^d} \tilde{\Phi}(k) \tilde{\rho}^*(k) \tilde{\Phi}(-k) - \int_{-\infty}^{\infty} \frac{d^d k}{(2\pi)^d} \tilde{\Phi}(-k) \tilde{\rho}^*(k) \frac{\tilde{\omega}(k)}{k^2} \tilde{J}(k) - W(J^2). \quad (2.43)$$

$W(J^2)$ denotes a Φ -independent term where the source only appears in second order and the inverse of $\rho^*(k)$ is the fixed point propagator

$$\frac{1}{\tilde{\rho}^*(k)} = \sum_{l \in \mathbf{Z}^d} \frac{\tilde{\omega}(k+2\pi l) \tilde{\omega}(-k-2\pi l)}{(k+2\pi l)^2} + \frac{1}{\kappa}. \quad (2.44)$$

The equation of motion to the fixed point action (2.43) in configuration space is the perfect Poisson equation

$$\sum_{n'} \rho^*(n-n') \Phi_{n'} = -J_n^{FP}. \quad (2.45)$$

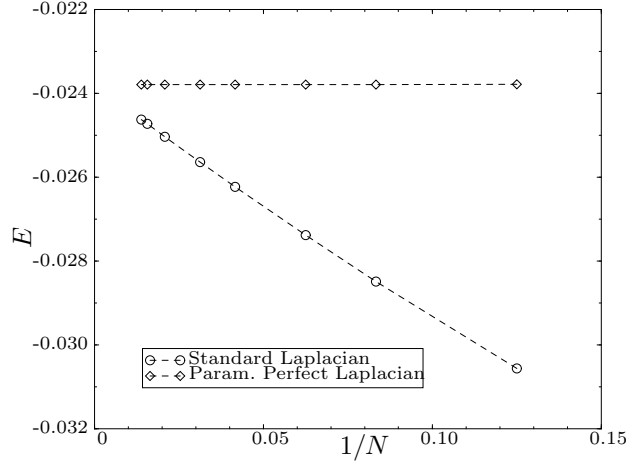


Figure 7: Comparison of the results for the potential energy of an L-shaped membrane between standard and parametrized perfect Laplacian. The error for the standard Laplacian is of order $1/N$.

with

$$\tilde{J}^{FP}(k) = \tilde{\rho}^*(k) \frac{\tilde{\omega}(k)}{k^2} \tilde{J}(k), \quad (2.46)$$

Therefore the perfect Laplace operator can be used to solve the Poisson equation with any source $J(x)$.

From Eq. (2.43) we can also read the fixed point field operator ϕ^{FP} which remains unchanged under RG transformations. Assume that the source $J(x)$ is small. Then the term of order J^2 can be neglected, and the transformation back to configuration space yields

$$\mathcal{A}[\Phi] = \frac{1}{2} \int_{-\pi}^{\pi} \frac{d^d k}{(2\pi)^d} \tilde{\Phi}(k) \tilde{\rho}^*(k) \tilde{\Phi}(-k) - \int d^d x J(x) \phi^{FP}(x). \quad (2.47)$$

The fixed point field operator is

$$\phi^{FP}(x) = \sum_n Z(x-n) \Phi_n, \quad (2.48)$$

with the coefficient function $Z(x)$ in configuration space

$$Z(x) = \int_{-\infty}^{\infty} \frac{d^d k}{(2\pi)^d} e^{-ikx} \tilde{\rho}^*(k) \frac{\tilde{\omega}(k)}{k^2}. \quad (2.49)$$

Using the fixed point field, we calculate the fixed point Laplacian in d dimensions for an arbitrarily placed $d-1$ -dimensional hyperplane as a boundary. Consider

zero boundary conditions $\phi(x) = 0, \forall x \in \Gamma$, where the boundary Γ divides the hyperspace into the halfspaces A inside and B outside the boundary (see Fig. 8 for $d = 2$). Start with the identity

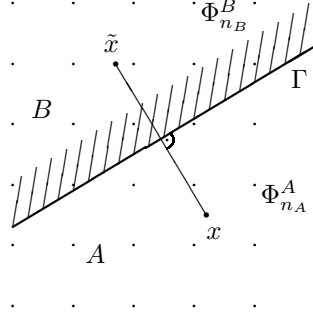


Figure 8: The line Γ as a boundary in $d = 2$. In the text we show how to calculate the perfect Laplacian restricted to the halfplane A .

$$\int d^d x (\phi(x) + \phi(\tilde{x}))^2 = 0, \quad (2.50)$$

which is trivially fulfilled because we impose the condition $\phi(\tilde{x}) = -\phi(x)$ on the field, where \tilde{x} denotes x mirrored at the boundary. If we plug the fixed point field (2.48), (2.49) into Eq. (2.50), we get the quadratic form $\Phi^T C \Phi = 0$, where Φ is the lattice field vector and the elements of the symmetric matrix C are

$$C_{nm} = \int d^d x [Z(x-n) + Z(\tilde{x}-n)][Z(x-m) + Z(\tilde{x}-m)]. \quad (2.51)$$

As it doesn't matter how we order the lattice points when arranging them in a vector, the lattice field vector Φ can be split into the subvectors Φ^A that collects all the components Φ_{n_A} living on the lattice points in halfspace A , and Φ^B that collects the components Φ_{n_B} in B . The quadratic form then gets

$$(\Phi^A)^T C_A \Phi^A + 2(\Phi^B)^T C_{BA} \Phi^A + (\Phi^B)^T C_B \Phi^B = 0, \quad (2.52)$$

where C_A , C_{BA} and C_B are submatrices of C

$$C = \begin{pmatrix} C_A & C_{AB} \\ C_{BA} & C_B \end{pmatrix}, \quad (2.53)$$

with $C_{BA} = C_{AB}^T$. Keeping Φ^A fixed and minimizing Eq. (2.52) in Φ^B , we find the relation between lattice points outside and inside the boundary $\Phi^B = -C_B^{-1} C_{BA} \Phi^A$. Plugging this into the perfect lattice Laplace equation $\sum_{n'} \rho^*(n-n') \Phi_{n'} = 0$, the sum over all lattice points n' is replaced by a sum over the halfspace A

$$\sum_{n'_A} \left[\rho^*(n-n'_A) - \sum_{n'_B} \rho^*(n-n'_B) (C_B^{-1} C_{BA})_{n'_B, n'_A} \right] \Phi_{n'_A} = 0, \quad (2.54)$$

and the perfect Laplacian $\rho_A^*(n_A, n'_A)$ restricted to the halfspace A is given by the term in square brackets. As the fixed point field operator is local, this exact result can be used to construct another parametrization of the fixed point Laplacian. The position and orientation of the hyperplane relative to the lattice are then the parameters and it only remains to calculate the couplings numerically.

8. Conclusion

The fixed point action has its applications not only in field theory, it can also serve as a powerful tool for the solution of partial differential equations, where we encounter non-trivial boundary conditions. We showed that the influence of boundaries on the fixed point action is highly local. Therefore we could provide a parametrization for the perfect lattice Laplace operator in $d = 2$ which is easy to use and gives nearly perfect results for any resolution. A generalization to d dimensions is trivial, as none of the calculations is specific to two dimensions. While the parametrization provided in this work can be used to approximate boundaries of any form, it is not the only one possible, and we proposed an alternative to find a parametrized fixed point Laplacian for non-trivial boundaries. The benefit from using perfect discretizations is enormous, as we pointed out for test problems.

Acknowledgments

I thank Peter Hasenfratz and Ferenc Niedermayer for their ideas and support during this work and Urs Wenger for his advice.

References

1. P. Hasenfratz and F. Niedermayer, *Nucl. Phys. B* **414**, 785 (1994).
2. K. G. Wilson and J. Kogut, *Phys. Rep. C* **12**, 75 (1974).
3. W. Bietenholz, hep-lat/9911015.
4. M. Blatter, R. Burkhalter, P. Hasenfratz and F. Niedermayer, *Nucl. Phys. B (Proc. Suppl.)* **42**, 799 (1995).
5. M. Blatter, R. Burkhalter, P. Hasenfratz and F. Niedermayer, *Phys. Rev. D* **53**, 923 (1996).
6. T. DeGrand, A. Hasenfratz, P. Hasenfratz and F. Niedermayer, *Nucl. Phys. B* **454**, 587 (1995); *ibid.* 615 (1995).
7. W. Bietenholz and U.-J. Wiese, *Nucl. Phys. B* **464**, 319 (1996).
8. W. Bietenholz and U.-J. Wiese, *Phys. Lett. B* **378**, 222 (1996).
9. C. B. Lang and T. K. Pany, *Nucl. Phys. B* **513**, 645 (1998).
10. F. Farchioni and V. Laliena, *Phys. Rev. D* **58** 054501 (1998) .
11. E. Katz and U.-J. Wiese, comp-gas/9709001.
12. T. L. Bell and K. G. Wilson, *Phys. Rev. B* **10**, 3935 (1974).
13. T. L. Bell and K. G. Wilson, *Phys. Rev. B* **11**, 3431 (1975).
14. P. Rufenacht, *The properties of the lattice fixed point action at different blockings*, Master's thesis, University of Bern, Switzerland, 1998.
15. K. G. Wilson, in *New Pathways in High Energy Physics II*, ed. A. Perlmutter (Plenum, New York 1976), p. 243.